

1 **REVISION 2**

2 **Thermodynamic investigation of uranyl vanadate minerals: implications for structural**  
3 **stability**

4 TYLER L. SPANO<sup>1\*</sup>, EWA A. DZIK<sup>1</sup>, MELIKA SHARIFIRONIZI<sup>1</sup>, MEGAN K. DUSTIN<sup>1</sup>, MADISON  
5 TURNER<sup>1</sup>, PETER C. BURNS<sup>1,2</sup>

6 <sup>1</sup>Department of Civil and Environmental Engineering and Earth Sciences, University of Notre  
7 Dame, Notre Dame, Indiana 46556

8 <sup>2</sup>Department of Chemistry and Biochemistry, University of Notre Dame, Notre Dame, Indiana  
9 46556

10  
11 **ABSTRACT**

12 Understanding the crystal chemistry, materials properties, and thermodynamics of uranyl  
13 minerals and their synthetic analogues is an essential step for predicting and controlling the long  
14 term environmental behavior of uranium. Uranyl vanadate minerals are relatively insoluble and  
15 widely disseminated within U ore deposits and mine and mill tailings. Pure uranyl vanadate  
16 mineral analogues were synthesized for investigation using high-temperature drop solution  
17 calorimetry. Calculated standard-state enthalpies of formation were found to be  $-4928.52 \pm$   
18  $13.90$ ,  $-5748.81 \pm 13.59$ , and  $-6402.88 \pm 21.01$ , kJ/mol for carnotite, curienite, and francevillite  
19 respectively. Enthalpies of formation from binary oxides for uranyl vanadate minerals exhibit a  
20 positive linear correlation as a function of the acidity of oxides. Normalized charge deficiency  
21 per anion (NCDA) is presented to relate bonding requirements of the structural units and  
22 interstitial complexes. An exponential correlation was observed between NCDA and energetic  
23 stability (enthalpy of formation from binary oxides) for the studied minerals. Additionally,  
24 NCDA and oxide acidity exhibit an exponential correlation where decreasing oxide acidity

25 results in an exponential decrease in NCDA. The number of occurrences of uranyl vanadate  
26 mineral species are found to correlate with both enthalpy of formation from oxides, and NCDA.

## 27 INTRODUCTION

28 In 1948, the US Atomic Energy Commission guaranteed a minimum price for uranium  
29 ore mined in the United States to decrease dependence on foreign sources (Brugge and Goble,  
30 2002). The resulting expansion of exploration and mining in the southwestern United States led  
31 to identification of over 7,000,000 tons of U ore (Brugge and Goble, 2002). Carnotite, ideally  
32  $K_2(UO_2)_2V_2O_8 \cdot 3H_2O$ , and other uranyl vanadate minerals, are widespread in U deposits of the  
33 American Southwest, and were thus especially important during this mining “boom”. Uranium  
34 and vanadium ore deposits located within the Uravan mineral belt in western Colorado and  
35 eastern Utah accounted for nearly 13% of the total U produced by the United States (Chenoweth,  
36 1981). In addition to the American Southwest, uranyl vanadate minerals originating from Africa  
37 were an important source of U for the development of both nuclear weapons and nuclear energy  
38 during and after World War II (Dumett, 1985). The solid solution series between curienite  
39  $(Pb(UO_2)_2V_2O_8 \cdot 5H_2O)$  and francevillite  $(Ba(UO_2)_2V_2O_8 \cdot 5H_2O)$  was first observed in samples  
40 from the mines of the Belgian Congo (now the Democratic Republic of the Congo), but has since  
41 been observed in other localities (Janeczek, 1999; Mereiter, 1986).

42 In the American Southwest and Africa, uranyl vanadate minerals are most common in  
43 areas where reduced uranium and reduced vanadium species are undergoing oxidation (Finch  
44 and Murakami, 1999). Primary U and V minerals that may alter to form uranyl vanadates include  
45 uraninite ( $UO_{2+x}$ ), montroseite  $(V^{3+}, Fe^{2+}, V^{4+})O(OH)$ , and davidite  
46  $(La(Y,U)Fe_2(Ti,Fe,Cr,V)_{18}(O,OH,F)_{38})$  (Krivovichev and Plášil, 2013; Weeks, 1961). Carnotite  
47 and other uranyl vanadates occur in Colorado Plateau-type U-V deposits, located on or near

48 fossil carbonaceous matter, and as alteration products in close proximity to uraninite (Dahlkamp,  
49 1993; Evans and Garrels, 1958).

50 Over a range of conditions, uranyl vanadate minerals are amongst the most insoluble  
51 alteration products of supergene U oxides, which are also significant ore sources (Barton, 1957;  
52 Krivovichev and Plášil, 2013; Plasil, 2014; Weeks, 1961). Owing to their insolubility, they retain  
53 uranium in natural systems. Between pH-Eh ranges of 4.5-8, and 1.0-0.0V, respectively,  
54 carnotite is stable, and uranyl vanadate minerals precipitate when dilute  $\text{UO}_2^{2+}$  and  $\text{VO}_4^{3-}$  are  
55 present in aqueous systems (Langmuir, 1978; Schindler et al., 2000). The solubility of carnotite  
56 in groundwater is very low, having been noted as being approximately 1ppb U in the pH range of  
57 5.5-7.5 (Barton, 1957). Carnotite precipitation from U-contaminated groundwater has been  
58 proposed as a potential method for treatment and remediation of groundwater and legacy wastes  
59 from mining operations (Tokunaga et al., 2009). A decrease in U concentrations in water below  
60 the drinking water standard of 30 ppb U, as outlined by the United States Environmental  
61 Protection Agency, was observed in batch experiments and calculations in which carnotite was  
62 precipitated (Tokunaga et al., 2009).

63 Over one century of research concerning uranyl vanadate minerals has yielded limited  
64 insight into the thermodynamic properties of these materials (Karyakin et al., 2003). Quantitative  
65 thermodynamic data are needed to define the relations between structural and energetic  
66 characteristics of these environmentally important phases (Karyakin et al., 2003). All uranyl  
67 vanadate minerals contain topologically identical uranyl vanadate sheets and substitution of  
68 interlayer cations is common. It has been suggested that the geometric arrangement of the  
69 interlayer cations is similar for all uranyl vanadate minerals, and thus does not substantially alter  
70 the stability of members of this group (Schindler et al., 2004b). Thermodynamic studies

71 presented here clarify the effect of structural arrangement and interlayer occupancy on the  
72 stabilities of mineral species that are chemically similar and occur in comparable geologic  
73 environments. Furthermore, investigating the thermodynamic properties of these minerals will  
74 aid in understanding the environmental behavior of U.

75 Previous studies have investigated the thermochemistry of some synthetic alkaline-earth  
76 uranyl vanadate mineral analogues (Karyakin et al., 2003). An adiabatic vacuum calorimeter was  
77 used to determine the heat capacities of synthetic crystalline alkaline-earth (Mg, Ca, Sr, and Ba)  
78 uranyl vanadates in the temperature range of 80-300K (Karyakin et al., 2003). High temperature  
79 calorimetry is necessary for rapid and reproducible data acquisition for refractory materials  
80 (Navrotsky, 1997). This technique is particularly applicable for enthalpy measurements of uranyl  
81 minerals as it ensures complete dissolution of materials regardless of chemical composition or  
82 structure (Shvareva et al., 2012).

### 83 STRUCTURES OF URANYL VANADATE MINERALS

84 Uranium is removed from primary minerals largely by oxidative dissolution, which forms  
85 the relatively soluble and environmentally mobile uranyl ion,  $\text{UO}_2^{2+}$  (Finch and Murakami,  
86 1999). Aqueous U(VI) chemistry is dominated by this near-linear uranyl ion. The uranyl moiety  
87 is ubiquitous in secondary uranium minerals and synthetic hexavalent uranium phases (Burns,  
88 2005). The formal charge of +2 on the uranyl ion requires further coordination by four, five, or  
89 six ligands in the equatorial planes of bipyramids about the uranyl. The coordination geometries  
90 include square, pentagonal, and hexagonal bipyramidal units (Burns, 2005). Owing to the uneven  
91 distribution of bond strengths in uranyl polyhedra, linkages through the equatorial ligands favor  
92 an abundance of sheet structures (Burns, 2005; Burns, 1997).

93 The sheets in the crystal structures of all uranyl vanadate minerals are topologically  
94 identical. In 2013, Krivovichev & Plasil (Krivovichev and Plášil, 2013) listed 13 naturally  
95 occurring uranyl vanadates (Table 1), all of which contain the  $[(\text{UO}_2)_2(\text{V}_2\text{O}_8)]^{2-}$  sheet that is  
96 based on the francevillite anion topology, and either mono, di, or tri-valent interstitial cations  
97 (Abraham et al., 1993; Cesbron and Morin, 1968; Mereiter, 1986). The anionic sheet possesses  
98  $\text{V}_2\text{O}_8$  dimers consisting of edge-sharing  $\text{V}^{5+}\text{O}_5$  square pyramidal units that are linked by uranyl  
99 ions in pentagonal bipyramidal coordination (Burns, 2005) (Figure 1). Neutrality is achieved by  
100 incorporation of interlayer cations between successive sheets. Hydration ranges from anhydrous  
101 to 11 water molecules per formula unit (Krivovichev and Plášil, 2013).

## 102 EXPERIMENTAL METHODS

### 103 Synthesis

104 Carnotite, francevillite, and curienite used in this study were synthesized through mild  
105 hydrothermal reactions of uranyl pyrovanadate (UPV) (Karyakin et al., 2000) and KOH,  
106  $\text{Ba}(\text{OH})_2$ , or  $\text{Pb}(\text{NO}_3)_2$ . UPV was synthesized by the high temperature solid-state reaction of  
107  $\text{NH}_4\text{VO}_3$  (MV Laboratories, 99.99%) and  $\gamma\text{-UO}_3$  (previously synthesized) (Appleman and Evans,  
108 1965; Requena Yáñez et al., 2012). To synthesize UPV, stoichiometric quantities of  $\text{NH}_4\text{VO}_3$   
109 and  $\text{UO}_3$  were weighed and ground together with acetone to promote homogeneity. The resulting  
110 powder was dried for 6 hours at  $150^\circ\text{C}$  and was then slowly heated in a Thermolyne 47900 box  
111 furnace to  $760^\circ$  over 12 hours, held at temperature for 72 hours, and then cooled to room  
112 temperature over another 72 hours (Karyakin et al., 2000). The resulting powder was identified  
113 as UPV by powder X-ray diffraction (Karyakin et al., 2000; Requena Yáñez et al., 2012).

114 To synthesize carnotite, 1.57g of UPV and 0.25g of KOH (Fisher, ACS grade) were  
115 weighed and ground together to ensure homogeneity. Approximately 450 mg of the mixture was  
116 placed in each of four Teflon-lined 23 mL Parr reaction vessels with 8 mL of 18 MΩ H<sub>2</sub>O in  
117 each. The pH of the mixture was initially between 12.3 and 12.4, and was adjusted to 2.3 by  
118 adding 0.4M HCl. Prior to all pH measurements, BDH Buffer Reference Standards were used  
119 for calibration. Similar methods were used to synthesize francevillite. For this, 1.57 g of UPV  
120 and 0.76g Ba(OH)<sub>2</sub> (Fisher, ACS grade) were weighed, ground, and divided evenly amongst 4  
121 reaction vessels. Upon addition of 8 mL of 18 MΩ H<sub>2</sub>O the pH of the mixtures ranged from 11.9  
122 to 12.5, and each was adjusted to 2.2 by adding 0.4M HCl. Curienite was synthesized by the  
123 reaction of 1.74g of UPV with 0.80g of Pb(NO<sub>3</sub>)<sub>2</sub> (Alfa Aesar, 99.99%). Reagents were weighed,  
124 ground, and placed in 4 reaction vessels with 8 mL 18 MΩ H<sub>2</sub>O in each. Initial pH values for  
125 these mixtures ranged from 2.9-3.5 and were adjusted to 2.3 by adding 0.4M HCl. For all  
126 hydrothermal reactions, limited initial solubility of reagents was observed.

127 The increase of temperature and pressure in the hydrothermal reactions promoted  
128 solubility of reagents and enabled formation of uranyl vanadate mineral analogues. After  
129 determining appropriate parameters from preliminary experiments, reaction vessels for all  
130 syntheses were sealed and placed in a Fisher Scientific Isotemp oven at 170°C for 5 days.  
131 Subsequent to cooling to room temperature, the products were recovered via vacuum filtration  
132 and rinsed with several aliquots of 18 MΩ H<sub>2</sub>O. No significant change in pH was observed  
133 following hydrothermal reactions.

134 Whereas uranyl vanadates are stable and form over a broad pH range, preliminary  
135 experiments had demonstrated that high purity material, as required for thermochemical studies,  
136 was obtained when the initial pH was adjusted to 2.2-2.3 (Barton, 1957; Karyakin et al., 2003;

137 Murata et al., 1949). As is commonly the case in hydrothermal synthesis, the exact speciation of  
138 U and V during the 5 day reaction time is not known. However, the aqueous speciation of both  
139 uranyl and vanadyl is strongly dependent on pH (Barton, 1957; Hostetler and Garrels, 1962).  
140 Under acidic conditions such as used here, U(VI) speciation is dominated by the uranyl ion,  
141 whereas vanadyl hydrolyzes significantly to form complex polyatomic species. (Gorman-Lewis  
142 et al., 2008; Hostetler and Garrels, 1962; Plasil, 2014; Weeks, 1961).

### 143 **Powder X-ray diffraction**

144 Powder X-ray diffraction data were collected using a Bruker D8 Advance Davinci  
145 powder diffractometer in Bragg-Brentano configuration. Cu-K $\alpha$  radiation was produced with an  
146 accelerating voltage of 40 kV and 40 mA current. An incident-beam slit of 1.0 mm was reduced  
147 by a 0.6 mm slit in combination with 0.02 mm absorber and diffraction (0.6 mm) slits. Data  
148 were collected using a step scan with a step velocity of 0.8° min<sup>-1</sup> in the range of 5-55 degrees 2 $\theta$   
149 using a LynxEye solid-state detector. Diffraction patterns all exhibited sharp profiles consistent  
150 with simulated powder diffraction patterns for carnotite, curienite, and francevillite, without  
151 additional peaks attributable to impurities.

### 152 **Chemical Analysis**

153 Chemical analyses were done using a Perkin Elmer Optima 8000 inductively coupled  
154 plasma-optical emission spectrometer (ICP-OES) with an analytical uncertainty of 3.5%.  
155 Analysis parameters were: 1400W torch power; nebulizer flow rate of 0.6 L/min; sample flow  
156 rate of 1.8 mL/min and a 45 second read delay. Approximately 25 mg of synthetic mineral  
157 powders were dissolved in 15 mL aqueous HNO<sub>3</sub> (5%) in triplicate. U, V, K, Ba, and Pb  
158 concentrations were determined using linear regression of seven standard solutions after

159 background subtraction. Calculated calibration coefficients were 0.99 or better for all elements of  
160 interest.

### 161 **Thermogravimetric analysis**

162 Thermogravimetric analyses were completed on a Netzsch TG209 F1 Iris thermal  
163 analyzer for ~25 mg aliquots of synthetic carnotite, curienite, and francevillite. Synthetic  
164 minerals were heated at 5°C/min from room temperature to 900°C under a stream of Ar gas at a  
165 rate of 50mL/min. Mass loss in the range of 30-105°C was assigned to the water present in each  
166 compound. No mass loss was observed for carnotite, indicating an anhydrous material as is  
167 typical of synthetic carnotite (Appleman and Evans, 1965). Observed mass loss for curienite and  
168 francevillite was in agreement with the chemical formulae  $\text{Pb}(\text{UO}_2)_2\text{V}_2\text{O}_8 \cdot 4.5\text{H}_2\text{O}$  and  
169  $\text{Ba}(\text{UO}_2)_2\text{V}_2\text{O}_8 \cdot 5\text{H}_2\text{O}$ , respectively. Limited quantities of analyzed material precluded analysis of  
170 final products after heating, although mixed U and V oxides are the likely result.

### 171 **Calorimetry**

172 Calorimetric data were collected using a Setaram AlexSys Calvet-type high-temperature  
173 calorimeter. Pellets of pressed synthetic carnotite, curienite, and francevillite weighing ~5mg  
174 were dropped from room temperature into the molten  $3\text{Na}_2\text{O}-4\text{MoO}_3$  solvent at 700°C under a  
175 stream of  $\text{O}_2$ . Complete dissolution of sample pellets in solvent was confirmed by visual  
176 inspection. The well-established heat content of  $\alpha\text{-Al}_2\text{O}_3$  was used as a calibrant (Shvareva et al.,  
177 2012). The measured enthalpies of drop solution,  $\Delta H_{\text{ds}}$ , were used to calculate enthalpies of  
178 formation using thermochemical cycles. Table 2 contains the thermochemical cycles for  
179 carnotite, curienite, and francevillite. The measured heat effect is the sum of heat capacity and



180 enthalpy of solution in the  $3\text{Na}_2\text{O}\text{-}4\text{MoO}_3$  solvent (Navrotsky, 1977; Navrotsky, 1997; Shvareva  
181 et al., 2012).

## 182 RESULTS

### 183 Enthalpies of reaction

184 The standard-state enthalpies of formation from the elements are  $-4928.52 \pm 13.90$  kJ/mol  
185 for carnotite,  $-5748.81 \pm 13.59$  kJ/mol for curienite, and  $-6402.88 \pm 21.01$  kJ/mol for  
186 francevillite. Calculated enthalpies of formation from binary oxides can be compared to reveal  
187 energetic trends of synthetic uranyl vanadate mineral analogues and are  $-566.62 \pm 12.11$ ,  $-244.70$   
188  $\pm 11.90$ , and  $-427.18 \pm 19.86$  kJ/mol for carnotite, curienite, and francevillite, respectively.  
189 Carnotite is thus more energetically favorable than curienite or francevillite when compared with  
190 the mechanical mixture of their constituent oxides.

191 Experimentally determined enthalpies of formation from binary oxides indicate that all  
192 uranyl vanadate minerals examined here are more energetically favorable than uranyl oxide  
193 hydrates, peroxides, phosphates, and silicates (Shvareva et al., 2012). The only uranyl minerals  
194 that are more energetically favorable with respect to calculated enthalpies of formation from  
195 binary oxides are the uranyl carbonates andersonite ( $\text{Na}_2\text{Ca}[(\text{UO}_2)(\text{CO}_3)_3]\cdot 5\text{H}_2\text{O}$ ) and grimselite  
196 ( $\text{K}_3\text{NaUO}_2(\text{CO}_3)_3\cdot 3\text{H}_2\text{O}$ ), with enthalpies of formation from binary oxides of  $-710.4 \pm 9.1$ , and -  
197  $989.3 \pm 14.0$  kJ $\cdot\text{mol}^{-1}$ , respectively (Navrotsky et al., 2013). The strongly negative formation  
198 enthalpies from oxides for uranyl carbonates has been attributed to robust acid-base interactions  
199 between acidic zero-dimensional uranyl tricarbonate clusters and basic interstitial cations Na, Ca,  
200 and K (Shvareva et al., 2012).

201 As carnotite, curienite, and francevillite contain identical uranyl vanadate sheets, it is  
202 possible to compare the contribution of acid-base interactions with counter cations to formation  
203 energetics. The interactions between charge-balancing cations and the  $[(\text{UO}_2)_2(\text{V}_2\text{O}_8)]^{2-}$  sheet are  
204 probed by plotting the measured formation enthalpies of oxides as a function of the acidity of the  
205 oxide as indexed on the Smith scale in which binary oxides have been assigned a numerical  
206 value based on stoichiometry (Smith, 1987). The observed linear relationship in Figure 2  
207 confirms the correlation between formation enthalpies from oxides and oxide acidity. Similar  
208 experimentally determined linear trends have been reported for uranyl silicates and uranyl  
209 hydroxide oxides (Navrotsky et al., 2013; Shvareva et al., 2012).

## 210 DISCUSSION

211 Structural stability, in addition to being quantified through thermodynamic  
212 measurements, can be inferred by comparing the balance of bond strengths between the  
213 structural unit and interstitial complexes (Hawthorne, 2012; Hawthorne, 2015; Hawthorne and  
214 Schindler, 2008; Schindler and Hawthorne, 2004; Schindler and Hawthorne, 2008). The  
215 structural unit of a crystalline solid is usually an anionic moiety of strongly bonded coordination  
216 polyhedra (Hawthorne, 2012). Interstitial complexes consist of lower-valence cations and water  
217 (Hawthorne, 2012). The number of bonds required by a structural unit can be estimated and  
218 related to its formal charge and number of O atoms (Hawthorne, 2012). The total number of  
219 bonds ( $\text{NB}_T$ ) in a structure is the sum of cation coordination numbers modified by the number of  
220 each cation in the chemical formula (Hawthorne, 2012). The number of bonds within the  
221 structural unit ( $\text{NB}_{\text{SU}}$ ) can be calculated in the same way, and the number of bonds required by  
222 the structural unit ( $\text{NB}_R$ ) is the difference between ( $\text{NB}_{\text{SU}}$ ) and ( $\text{NB}_T$ ) (Hawthorne, 2012). Using  
223 this method,  $\text{NB}_T$  and  $\text{NB}_R$  have been calculated for carnotite, curienite, and francevillite.

224           The number of bonds required ( $NB_R$ ) by the structural unit can be further modified by  
225 calculating the charge deficiency per anion (CDA). CDA is calculated by dividing the formal  
226 charge (FC) of the structural unit by the number of oxygen atoms ( $N_o$ ) within the structural unit  
227 (Schindler and Hawthorne, 2008). In all uranyl vanadate minerals,  $FC = -2$  and  $N_o = 12$ , therefore  
228 the CDA for all uranyl vanadate minerals is 0.166 valence units (v.u.) (Schindler et al., 2004a;  
229 Schindler et al., 2004b). The charge deficiency per anion may be normalized, for the purpose of  
230 comparison across different structures, by dividing by  $NB_R$ , yielding the normalized charge  
231 deficiency per anion (NCDA). Calculated NCDA values for carnotite, curienite, and francevillite  
232 are 0.0093, 0.0208, and 0.0185 v.u. respectively. Experimentally determined enthalpies of  
233 formation plotted as a function of NCDA in Figure 3, reveals an exponential decrease in stability  
234 (less-negative  $\Delta H_{f-ox}$ ) as NCDA increases. NCDA is a measure of the degree of unsatisfied  
235 bonding of the structural unit and structure stability depends on the degree to which this can be  
236 accounted for by linkages to the interstitial complex. This model confirms that a higher degree of  
237 unsatisfied bonding requirements correlates exponentially to a decrease in energetic favorability.

238           Oxide acidity of the interstitial complex is exponentially related to calculated NCDA  
239 values. Decreasing oxide acidity results in an exponential decrease in normalized charge  
240 deficiency per anion. This observation, coupled with the relationship between oxide acidity and  
241 enthalpy of formation from oxides clarifies the relation between structure and thermodynamics.  
242 Correlations between NCDA and energetics have yet to be investigated in other mineral systems  
243 that have identical structural units.

244

245

246

## IMPLICATIONS

247           Observed enthalpies of formation for carnotite, curienite, and francevillite indicate that  
248 uranyl vanadate phases are energetically stable relative to the oxides at 298 K. Each of these  
249 minerals contain identical uranyl vanadate sheets, and differences in stabilities therefore relate to  
250 the identity and bonding behavior of interstitial complexes. There is an exponential relationship  
251 between the enthalpies of formation of these minerals from the oxides and the normalized charge  
252 deficiency of the anions in the structural unit. This confirms the importance of charge density  
253 matching between the structural unit and interstitial complex in determining the thermodynamic  
254 properties of these minerals. In addition to element availability in a given set of geochemical  
255 conditions, these energetic considerations impact mineral occurrences.

256

## ACKNOWLEDGEMENTS

257           We thank Editor Julien Mercadier, referee Michael Schindler and an anonymous referee  
258 for their insightful comments on this paper, and Lei Zhang for her assistance with  
259 thermodynamic calculations. This research is supported by the Materials Science of Actinides  
260 Center, an Energy Frontier Research Center funded by the U.S. Department of Energy, Office of  
261 Science, Office of Basic Energy Sciences under Award Number DE-SC0001089. Partial support  
262 of this project is from the Patrick and Jana Eilers graduate student fellowship. Chemical analyses  
263 were conducted at the Center for Environmental Science and Technology, and the ND Energy  
264 Materials Characterization Facility at the University of Notre Dame.

265

266

267

268

269 **Figures and Tables**

270 **TABLE 1.** Recognized Uranyl Vanadate Mineral Species

271 Modified from Krivovichev and Plášil (Krivovichev and Plášil, 2013)

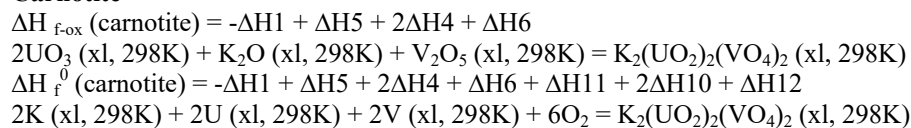
Chemical Formula	Mineral Name	Space Group	$a[\text{Å}]/\alpha[^\circ]$	$b[\text{Å}]/\beta[^\circ]$	$c[\text{Å}]/\gamma[^\circ]$
$\text{Cu}[(\text{UO}_2)_2(\text{V}_2\text{O}_8)](\text{OH})(\text{H}_2\text{O})_3$	sengierite	$P2_1/a$	10.60/ 90	8.09/ 103.4	10.09/ 90
$\text{K}_2[(\text{UO}_2)_2(\text{V}_2\text{O}_8)]$	carnotite	$P2_1/a$	10.47/ 90	8.42/ 103.8	6.59/ 90
$\text{Cs}_2[(\text{UO}_2)_2(\text{V}_2\text{O}_8)]$	margaritasite	$P2_1/a$	10.51/ 90	8.45/ 106.1	7.32/ 90
$\text{Pb}[(\text{UO}_2)_2(\text{V}_2\text{O}_8)](\text{H}_2\text{O})_5$	curienite	$Pcan$	10.42/ 90	8.49/ 90	16.41/ 90
$\text{Ba}[(\text{UO}_2)_2(\text{V}_2\text{O}_8)](\text{H}_2\text{O})_5$	francevillite	$Pcan$	10.48/ 90	8.45/ 90	16.65/ 90
$\text{Ca}[(\text{UO}_2)_2(\text{V}_2\text{O}_8)](\text{H}_2\text{O})_8$	tyuyamunite	$Pnna$	10.63/ 90	8.36/ 90	20.40/ 90
$\text{Ca}[(\text{UO}_2)_2(\text{V}_2\text{O}_8)](\text{H}_2\text{O})_5$	metatyuyamunite	$O^*$	10.63/ 90	8.36/ 90	16.96/ 90
$\text{Al}[(\text{UO}_2)_2(\text{V}_2\text{O}_8)](\text{OH})(\text{H}_2\text{O})_{11}$	vanuralite	$M^*$	10.33/ 90	8.44/ 103.0	24.52/ 90
$\text{Al}[(\text{UO}_2)_2(\text{V}_2\text{O}_8)](\text{OH})(\text{H}_2\text{O})_8$	metavanuralite	$P-1$	10.46/ 75.9	8.44/ 102.8	10.43/ 90
$\text{Na}_2[(\text{UO}_2)_2(\text{V}_2\text{O}_8)](\text{H}_2\text{O})_5$	strelkinite	$Pnmm$	10.64/ 90	8.36/ 90	32.73/ 90
$\text{Na}_2[(\text{UO}_2)_2(\text{V}_2\text{O}_8)](\text{H}_2\text{O})_2$	metastrelkinite I	$P2_1/n$	10.50/ 90	8.28/ 97.6	16.24/ 90
$\text{Na}_2[(\text{UO}_2)_2(\text{V}_2\text{O}_8)](\text{H}_2\text{O})_2$	metastrelkinite II	$P2_1/a$	10.48/ 90	8.51/ 113.2	7.72/ 90
$\text{Na}_2[(\text{UO}_2)_2(\text{V}_2\text{O}_8)]$	metastrelkinite III	$P2_1/a$	10.42/ 90	8.34/ 100.5	6.02/ 90

272 \* Space group unknown.  $O$ = orthorhombic,  $M$ = monoclinic

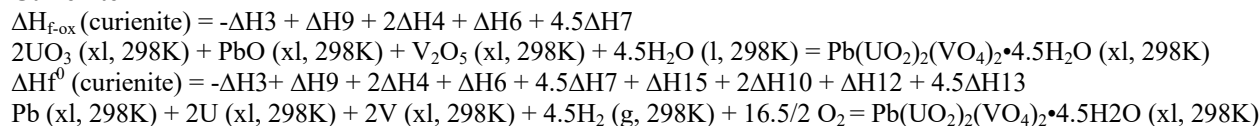
273

274 **TABLE 2.** Calorimetric cycles for enthalpy of formation calculations for uranyl vanadate minerals

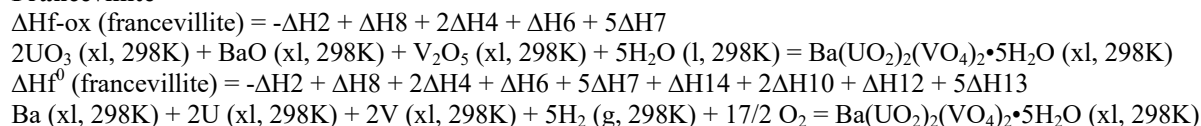
**Carnotite**



**Curienite**

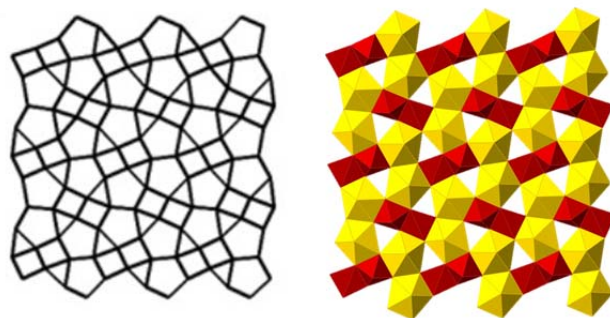


**Francevillite**



Reactions	$\Delta H$ (kJ/mol)	$\Delta H$ (kJ/mol)	$\Delta H$ (kJ/mol)	REF
1	$\Delta H_{ds}$ (Carnotite)	$\text{K}_2(\text{UO}_2)_2(\text{VO}_4)_2(\text{xl}, 298\text{K}) = \text{K}_2\text{O}(\text{soln}, 976\text{K}) + 2\text{UO}_3(\text{soln}, 976\text{K}) + \text{V}_2\text{O}_5(\text{soln}, 976\text{K})$	$407.62 \pm 11.12$	
2	$\Delta H_{ds}$ (Francevillite)	$\text{Ba}(\text{UO}_2)_2(\text{VO}_4)_2 \cdot 5\text{H}_2\text{O}(\text{xl}, 298\text{K}) = \text{BaO}(\text{soln}, 976\text{K}) + 2\text{UO}_3(\text{soln}, 976\text{K}) + \text{V}_2\text{O}_5(\text{soln}, 976\text{K}) + 5\text{H}_2\text{O}(\text{g}, 976\text{K})$	$746.58 \pm 19.26$	
3	$\Delta H_{ds}$ (Curienite)	$\text{Pb}(\text{UO}_2)_2(\text{VO}_4)_2 \cdot 4.5\text{H}_2\text{O}(\text{xl}, 298\text{K}) = \text{PbO}(\text{soln}, 976\text{K}) + 2\text{UO}_3(\text{soln}, 976\text{K}) + \text{V}_2\text{O}_5(\text{soln}, 976\text{K}) + 4.5\text{H}_2\text{O}(\text{g}, 976\text{K})$	$698.80 \pm 11.27$	
4	$\Delta H_{ds}$ (UO <sub>3</sub> )	$\text{UO}_3(\text{xl}, 298\text{K}) = \text{UO}_3(\text{soln}, 976\text{K})$	$9.5 \pm 1.50$	(Helean et al., 2002)
5	$\Delta H_{ds}$ (K <sub>2</sub> O)	$\text{K}_2\text{O}(\text{xl}, 298\text{K}) = \text{K}_2\text{O}(\text{soln}, 976\text{K})$	$-318 \pm 3.10$	(Molodetsky et al., 2000)
6	$\Delta H_{ds}$ (V <sub>2</sub> O <sub>5</sub> )	$\text{V}_2\text{O}_5(\text{xl}, 298\text{K}) = \text{V}_2\text{O}_5(\text{soln}, 976\text{K})$	$140 \pm 2.10$	(Navrotsky, 2014)
7	$\Delta H_{hc}$ (H <sub>2</sub> O)	$\text{H}_2\text{O}(\text{l}, 298\text{K}) = \text{H}_2\text{O}(\text{g}, 976\text{K})$	$69 \pm 0$	(Robie and Hemingway, 1995)
8	$\Delta H_{ds}$ (BaO)	$\text{BaO}(\text{xl}, 298\text{K}) = \text{BaO}(\text{soln}, 976\text{K})$	$-184.6 \pm 3.2$	(Robie and Hemingway, 1995)
9	$\Delta H_{ds}$ (PbO)	$\text{PbO}(\text{xl}, 298\text{K}) = \text{PbO}(\text{soln}, 976\text{K})$	$-15.4 \pm 1.10$	(Navrotsky, 2014)
10	$\Delta H_f^0$ (UO <sub>3</sub> )	$\text{U}(\text{xl}, 298\text{K}) + 3/2 \text{O}_2(\text{g}, 298\text{K}) = \text{UO}_3(\text{xl}, 298\text{K})$	$-1224 \pm 0.80$	(Robie and Hemingway, 1995)
11	$\Delta H_f^0$ (K <sub>2</sub> O)	$2\text{K}(\text{xl}, 298\text{K}) + 1/2 \text{O}_2(\text{g}, 298\text{K}) = \text{K}_2\text{O}(\text{xl}, 298\text{K})$	$-363.2 \pm 2.10$	(Robie and Hemingway, 1995)
12	$\Delta H_f^0$ (V <sub>2</sub> O <sub>5</sub> )	$2\text{V}(\text{xl}, 298\text{K}) + 5/2 \text{O}_2(\text{g}, 298\text{K}) = \text{V}_2\text{O}_5(\text{xl}, 298\text{K})$	$-1550.6 \pm 6.30$	(Robie and Hemingway, 1995)
13	$\Delta H_f^0$ (H <sub>2</sub> O)	$\text{H}_2(\text{g}, 298\text{K}) + 1/2 \text{O}_2(\text{g}, 298\text{K}) = \text{H}_2\text{O}(\text{l}, 298\text{K})$	$-285.8 \pm 0.10$	(Robie and Hemingway, 1995)
14	$\Delta H_f^0$ (BaO)	$\text{Ba}(\text{xl}, 298\text{K}) + 1/2 \text{O}_2(\text{g}, 298\text{K}) = \text{BaO}(\text{xl}, 298\text{K})$	$-548.1 \pm 2.10$	(Robie and Hemingway, 1995)
15	$\Delta H_f^0$ (PbO)	$\text{Pb}(\text{xl}, 298\text{K}) + 1/2 \text{O}_2(\text{g}, 298\text{K}) = \text{PbO}(\text{xl}, 298\text{K})$	$-219.41 \pm 0.80$	(Robie and Hemingway, 1995)

275 **FIGURE 1.** The francevillite anion topology (left) and population of the francevillite anion  
276 topology (right) by pentagonal bipyramids of uranium and square pyramids of vanadium.  
277 Modified from Burns (Burns, 2005).



278

279

280

281

282

283

284

285

286

287

288

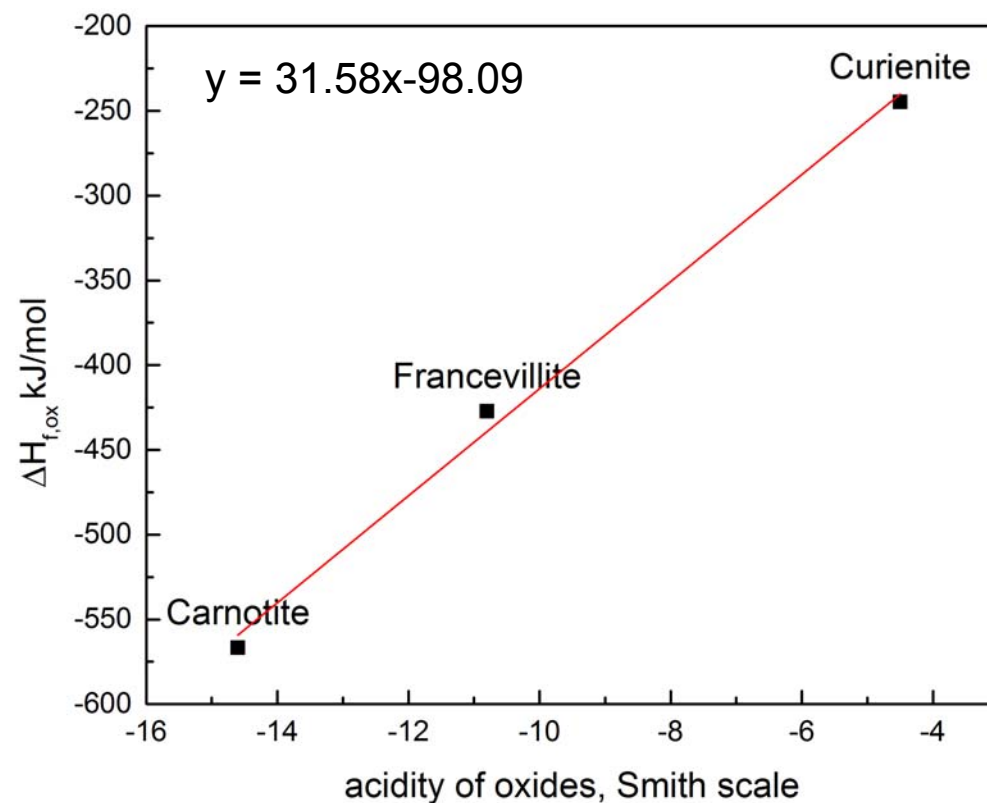
289

290

291

292

293 **FIGURE 2.** Enthalpies of formation from oxides for carnotite, curienite, and francevillite as a  
294 function of acidity of oxides (Smith, 1987).



295

296

297

298

299

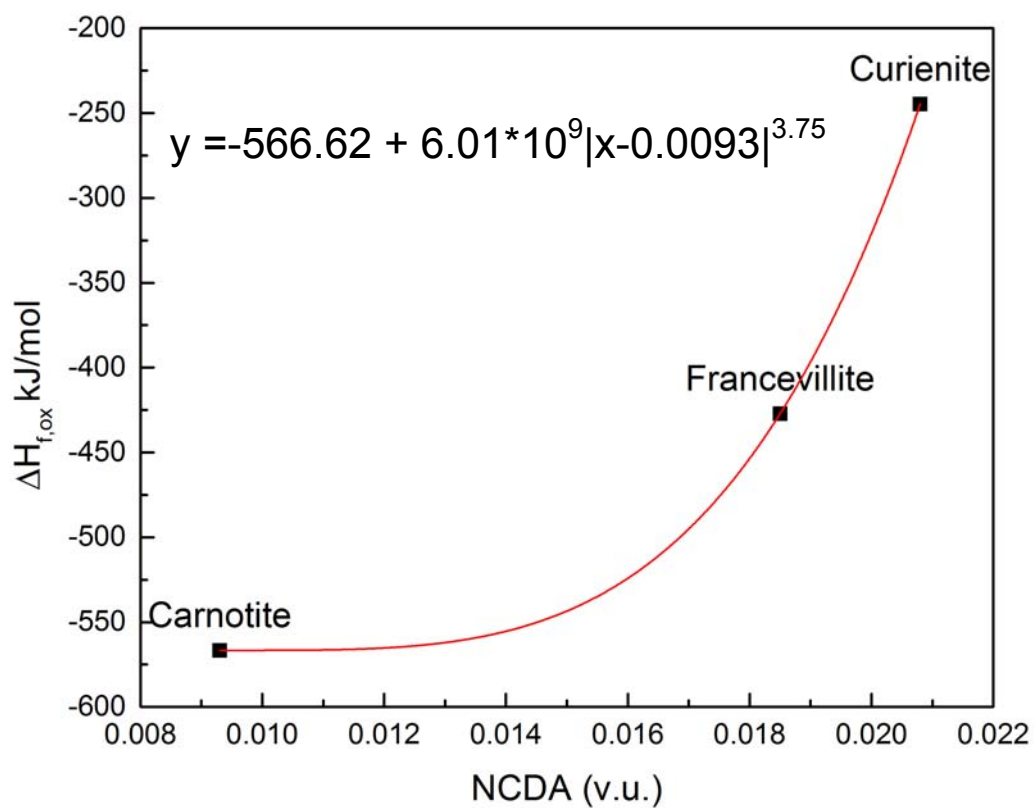
300

301



302

303 **FIGURE 3.** Enthalpies of formation from oxides for carnotite, curienite, and francevillite as a  
304 function of normalized charge deficiency per anion (NCDA).



305

306

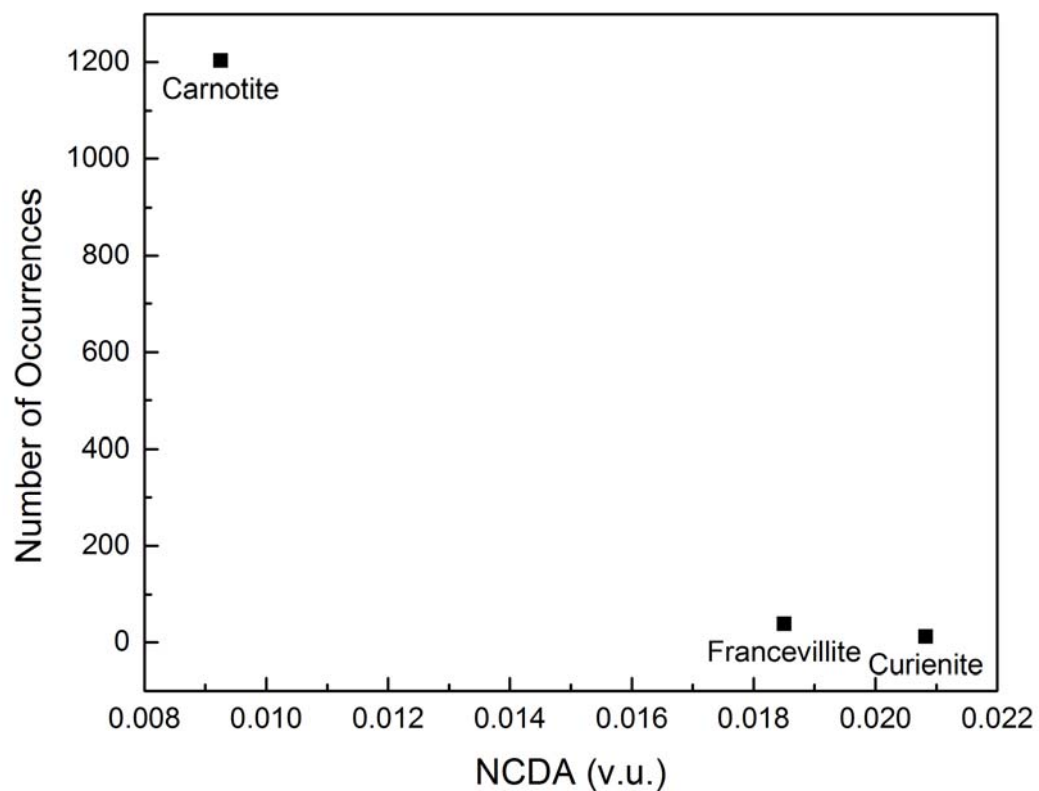
307

308

309

310

311 **FIGURE 4.** Number of occurrences (2016) plotted as a function of NCDA.



312  
313  
314  
315  
316  
317  
318  
319  
320  
321  
322  
323

- 325 Mindat.org (2016), p. <http://www.mindat.org/min-907.html>, <http://www.mindat.org/min-1196.html>, <http://www.mindat.org/min-1589.html>. Hudson Institute of Mineralogy.
- 326
- 327 Abraham, F., Dion, C., and Saadi, M. (1993) Carnotite analogues: synthesis, structure and  
328 properties of the  $\text{Na}_1\text{-K}\text{UO}_2\text{VO}_4$  solid solution ( $0 \leq x \leq 1$ ). *Journal of Materials Chemistry*,  
329 3(5), 459-463.
- 330 Appleman, D.E., and Evans, H. (1965) The crystal structures of synthetic anhydrous carnotite,  
331  $\text{K}_2(\text{UO}_2)_2\text{V}_2\text{O}_8$ , and its cesium analogue,  $\text{Cs}_2(\text{UO}_2)_2\text{V}_2\text{O}_8$ . *Am. Mineral*, 50(7), 8.
- 332 Barton, P.B. (1957) Synthesis and properties of carnotite and its alkali analogues. *Trace*  
333 *Elements Investigations*.
- 334 Brugge, D., and Goble, R. (2002) The History of Uranium Mining and the Navajo People.  
335 *American Journal of Public Health*, 92(9), 1410-1419.
- 336 Burns, P.C. (2005)  $\text{U}^{6+}$  minerals and inorganic compounds: insights into an expanded structural  
337 hierarchy of crystal structures. *The Canadian Mineralogist*, 43(6), 1839-1894.
- 338 Burns, P.C.E., R. C.; Hawthorne, F.C. (1997) The crystal chemistry of hexavalent uranium:  
339 Polyhedron geometries, bond-valence parameters and polymerization polyhedra. *The*  
340 *Canadian Mineralogist*, 35.
- 341 Cesbron, F., and Morin, N. (1968) Curienite, a new mineral species. A study of the series  
342 francevillite-curienite. *Laboratoire de Mineralogie-Cristallographie, Paris*.
- 343 Chenoweth, W.L. (1981) The uranium-vanadium deposits of the UraVan Mineral Belt and  
344 adjacent areas, Colorado and Utah. *New Mexico Geological Society 32nd Annual Fall*  
345 *Field Conference Guidebook*, p. 165-170.
- 346 Dahlkamp, F.J. (1993) *Uranium Ore Deposits*. Springer-Verlag.
- 347 Dumett, R. (1985) Africa's strategic minerals during the Second World War. *The Journal of*  
348 *African History*, 26(4), 381-408.
- 349 Evans, H.T., and Garrels, R.M. (1958) Thermodynamic equilibria of vanadium in aqueous  
350 systems as applied to the interpretation of the Colorado Plateau ore deposits. *Geochimica*  
351 *et Cosmochimica Acta*, 15(1), 131-149.
- 352 Finch, R., and Murakami, T. (1999) Systematics and paragenesis of uranium minerals. *Reviews*  
353 *in Mineralogy and Geochemistry*, 38(1), 91-179.
- 354 Gorman-Lewis, D., Burns, P.C., and Fein, J.B. (2008) Review of uranyl mineral solubility  
355 measurements. *The Journal of Chemical Thermodynamics*, 40(3), 335-352.
- 356 Hawthorne, F.C. (2012) A bond-topological approach to theoretical mineralogy: crystal  
357 structure, chemical composition and chemical reactions. *Physics and Chemistry of*  
358 *Minerals*, 39(10), 841-874.
- 359 -. (2015) Roebbling Medal Paper. Toward theoretical mineralogy: A bond-topological approach.  
360 *American Mineralogist*, 100(4), 696-713.
- 361 Hawthorne, F.C., and Schindler, M. (2008) Understanding the weakly bonded constituents in  
362 oxysalt minerals. *Zeitschrift für Kristallographie*, 223(01-02), 41-68.
- 363 Helean, K., Navrotsky, A., Vance, E., Carter, M., Ebbinghaus, B., Krikorian, O., Lian, J., Wang,  
364 L., and Catalano, J. (2002) Enthalpies of formation of Ce-pyrochlore,  
365  $\text{Ca}_{0.93}\text{Ce}_{1.00}\text{Ti}_{2.035}\text{O}_{7.00}$ , U-pyrochlore,  $\text{Ca}_{1.46}\text{U}^{4+}_{0.23}\text{U}^{6+}_{0.46}\text{Ti}_{1.85}\text{O}_{7.00}$  and Gd-pyrochlore,  
366  $\text{Gd}_2\text{T}_2\text{O}_7$ : three materials relevant to the proposed waste form for excess weapons  
367 plutonium. *Journal of Nuclear Materials*, 303(2), 226-239.

- 368 Hostetler, P.B., and Garrels, R.M. (1962) Transportation and precipitation of uranium and  
369 vanadium at low temperatures, with special reference to sandstone-type uranium deposits.  
370 Economic Geology and the Bulletin of the Society of Economic Geologists, 57(2), 137-  
371 167.
- 372 Janeczek, J. (1999) Mineralogy and geochemistry of natural fission reactors in Gabon. Reviews  
373 in Mineralogy and Geochemistry, 38(1), 321-392.
- 374 Karyakin, N., Chernorukov, N., Suleimanov, E., and Alimzhanov, M. (2003) Chemical  
375 thermodynamics of alkaline-earth metal uranovanadates. Radiochemistry, 45(5), 457-  
376 468.
- 377 Karyakin, N.V., Chernorukov, N.G., Sulejmanov, E.V., Alimzhanov, M.I., Trostin, V.L., and  
378 Knyazev, A.V. (2000) The thermodynamic properties of uranyl pyrovanadate and  
379 uranovanadic acid. Zhurnal Fizicheskoy Khimii, 74(8), 1366-1371.
- 380 Krivovichev, S.V., and Plášil, J. (2013) Mineralogy and crystallography of uranium. Uranium:  
381 From Cradle to Grave. Mineralogical Association of Canada Short Courses, 43, 15-119.
- 382 Langmuir, D. (1978) Uranium solution-mineral equilibria at low temperatures with applications  
383 to sedimentary ore deposits. Geochimica et Cosmochimica Acta, 42(6), 547-569.
- 384 Mereiter, K. (1986) Crystal structure refinements of two francevillites, (Ba, Pb)[(UO<sub>2</sub>)<sub>2</sub>V<sub>2</sub>O<sub>8</sub>]·  
385 5H<sub>2</sub>O. Neues Jahrbuch für Mineralogie-Monatshefte, 1986, 552-560.
- 386 Molodetsky, I., Navrotsky, A., DiSalvo, F., and Lerch, M. (2000) Energetics of oxidation of  
387 oxynitrides: Zr-N-O, Y-Zr-N-O, Ca-Zr-N-O, and Mg-Zr-N-O. Journal of Materials  
388 Research, 15(11), 2558-2570.
- 389 Murata, K.J., Cisney, E.A., Stieff, L.R., and Zworykin, E.V. (1949) Synthesis, Base Exchange,  
390 and Photosensitivity of Carnotite, Tyuyamunite, and Related Minerals. Trace Elements  
391 Investigations.
- 392 Navrotsky, A. (1977) Progress and new directions in high temperature calorimetry. Physics and  
393 Chemistry of Minerals, 2(1), 89-104.
- 394 -. (1997) Progress and new directions in high temperature calorimetry revisited. Physics and  
395 Chemistry of Minerals, 24(3), 222-241.
- 396 -. (2014) Progress and new directions in calorimetry: A 2014 perspective. Journal of the  
397 American Ceramic Society, 97(11), 3349-3359.
- 398 Navrotsky, A., Shvareva, T., and Guo, X. (2013) Thermodynamics of uranium minerals and  
399 related materials. In P.C. Burns, and G.E. Sigmon, Eds. Uranium: Cradle to Grave, 43, p.  
400 147-164. Mineralogical Association of Canada, Winnipeg, Manitoba.
- 401 Plasil, J. (2014) Oxidation-hydration weathering of uraninite: the current state-of-knowledge.  
402 Journal of Geosciences, 59(2), 99-114.
- 403 Requena Yáñez, J., Reyes Cortés, M., Torres Moye, E., Lardizabal, D., Riveros, H., and Montero  
404 Cabrera, M. (2012) Synthesis of potassium and calcium uranovanadates, analogues of  
405 carnotite and metatyuyamunite minerals. Revista mexicana de física, 58(3), 253-257.
- 406 Robie, R.A., and Hemingway, B.S. (1995) Thermodynamic properties of minerals and related  
407 substances at 298.15 K and 1 bar (10<sup>5</sup> pascals) pressure and at higher temperatures.  
408 Bulletin.
- 409 Schindler, M., and Hawthorne, F.C. (2004) A bond-valence approach to the uranyl-oxide  
410 hydroxy-hydrate minerals: chemical composition and occurrence. The Canadian  
411 Mineralogist, 42(6), 1601-1627.
- 412 -. (2008) The stereochemistry and chemical composition of interstitial complexes in uranyl-  
413 oxysalt minerals. . The Canadian Mineralogist, 46(2), 467-501.

- 414 Schindler, M., Hawthorne, F.C., and Baur, W.H. (2000) A crystal-chemical approach to the  
415 composition and occurrence of vanadium minerals The Canadian Mineralogist, 38(6),  
416 1443-1456.
- 417 Schindler, M., Mutter, A., Hawthorne, F.C., and Putnis, A. (2004a) Prediction of crystal  
418 morphology of complex uranyl-sheet minerals. I. Theory. The Canadian Mineralogist,  
419 42(6), 1629-1649.
- 420 -. (2004b) Prediction of crystal morphology of complex uranyl-sheet minerals. II. Observations.  
421 The Canadian Mineralogist, 42(6), 1651-1666.
- 422 Shvareva, T.Y., Fein, J.B., and Navrotsky, A. (2012) Thermodynamic properties of uranyl  
423 minerals: Constraints from calorimetry and solubility measurements. Industrial &  
424 Engineering Chemistry Research, 51(2), 607-613.
- 425 Smith, D.W. (1987) An acidity scale for binary oxides. Journal of Chemical Education, 64(6),  
426 480.
- 427 Tokunaga, T.K., Kim, Y., and Wan, J. (2009) Potential remediation approach for uranium-  
428 contaminated groundwaters through potassium uranyl vanadate precipitation.  
429 Environmental Science & Technology, 43(14), 5467-5471.
- 430 Weeks, A.D. (1961) Mineralogy and geochemistry of vanadium in the Colorado Plateau. Journal  
431 of the Less Common Metals, 3(6), 443-450.

432